PREPRINT UCRL-79642 (Rev. 1)

CONF-770644--6

Lawrence Livermore Laboratory

DIRECT ENERGY CONVERSION AND NEUTRAL BEAM INJECTION FOR CATALYZED D AND D-^{3}He TOKAMAK REACTORS

Asher S. Blum, Ralph W. Moir

July 7, 1977

This paper was prepared for submission to the Electric Power Research Institute Review Meeting on Advanced Fuel Fusion, Chicago, Ill., June 27-29, 1977

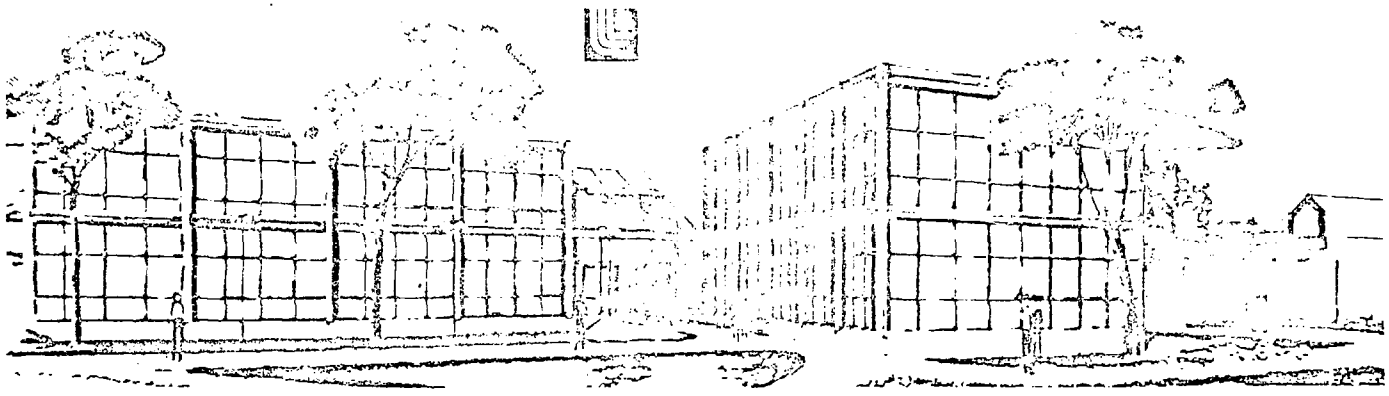

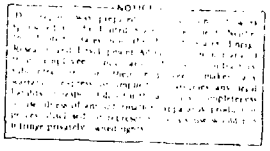

Direct Energy Conversion and Neutral Beam Injection for Catalyzed D and D - ^{3}He Tokamak Reactors*

by

Asher S. Blum and Ralph W. Moir
Lawrence Livermore Laboratory
P.O. Box 808
Livermore, California 94550

ABSTRACT

The calculated performance of single stage and Venetian blind direct energy converters for Catalyzed D and D - ^{3}He Tokamak reactors are discussed. Preliminary results on He pumping are outlined. The efficiency of D and T neutral beam injection is reviewed.

*Performed for the Electric Power Research Institute under Contract No. RP645-2 and under the auspices of the U.S. Energy Research and Development Administration under Contract No. W-7405-Eng-48.

I. INTRODUCTION

D-D and D-^{3}He fusion reactions yield a large fraction of their energy as energetic charged particles. In order to assess the potential benefit, we have studied the performance and technology requirements of direct energy converters when attached to such advanced fueled reactors. Direct converters can recover a portion of the charged-particle energy directly and send most of the remainder (in the form of heat) to a thermal bottoming cycle. Depending, of course, upon the ion energy distribution and the recovery technology, Venetian blind direct converter efficiencies as high as 65% have been calculated for more conventional, D-T fueled reactors. Our purpose was to extend these studies to Cat-D and D-^{3}He machines[1]; we will present the calculated results.

The problems of fueling and heating plasmas by the neutral beam injection of deuterium and tritium has been extensively studied; the method appears to be practical in the case of Tokamaks. We will discuss the efficiencies that can be expected.

II. DIRECT ENERGY CONVERSION

We begin with a brief review of the types of direct energy converters that were studied. A Tokamak reactor is assumed.

- A portion of the Tokamak plasma diffuses across magnetic field lines until it encounters a line that leaves the reactor interior through a bundle divertor.
- The plasma follows the field line out of the reactor and enters a conical "expander" tank several 10's of meters long, such as is shown in Fig. 1.
- Because of the magnetic mirror-like action of the divertor coil, the reactor plasma on the field lines linked by the divertor coil will be at a positive ambipolar potential with respect to the reactor wall. As plasma travels toward the grounded grid

---

[1] In particular, we considered direct energy conversion on five different reactor designs, developed by the University of Illinois and BNL.

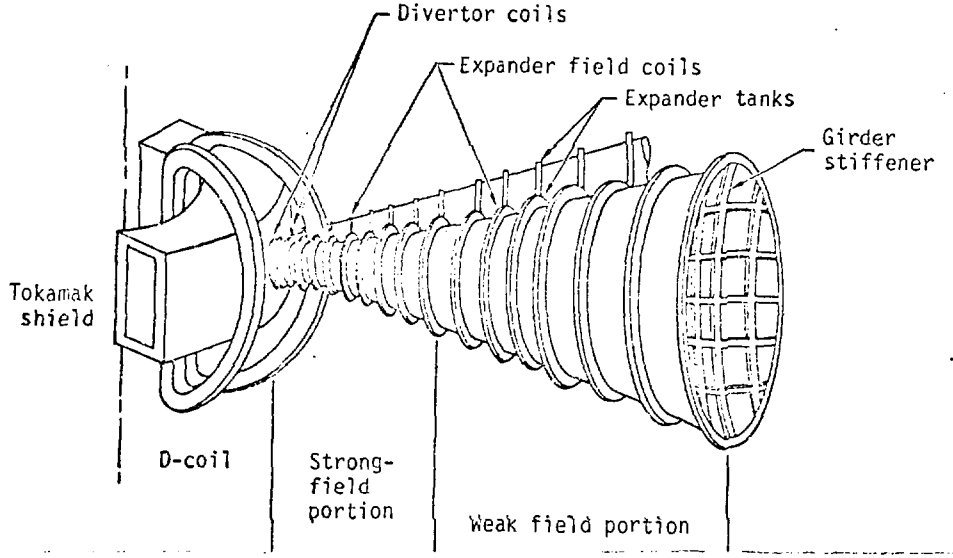

Figure 1. A pair of expander tanks are sketched along with a portion of the Tokamak reactor.

at the far end of the tank, the ions will be accelerated by this potential; the electrons will be slowed down.

- The plasma stream expands along field lines as it travels down the tank. This implies a decreasing magnetic field, which in turn converts the ion velocity component, $V_{\perp}$, into $V_{\parallel}$. The charged particle power density and the charged particle density are both reduced.
- Near the wider, far end of the tank, the direct converter electrodes are encountered. These are shown in Fig. 2. Some of the electrons (a number equal to the ion current) strike the grounded grid and are removed. The remaining electrons are reflected back toward the reactor by the negative grid.
- The ions are accelerated between grids, but slow down in velocity after they pass the negative grid and approach the electrically positive collector.
- The slowed down ions strike the positive collector. Their excess energy is given up as heat.

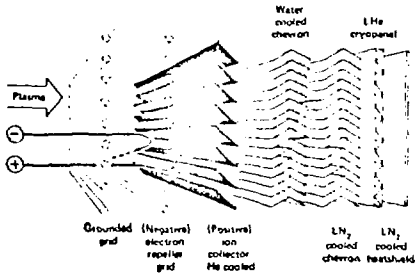

Figure 2. The single-stage direct converter electrode structure

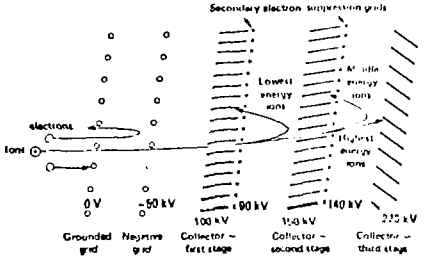

Figure 3. The three-stage Venetian blind direct converter electrode structure

The multistage collector shown in Fig. 3 can be used to increase the electrical output. The higher energy ions are collected on high voltage collectors. Their excess energy, upon collection, is smaller. More electrical power and less heat is produced.

III. MODELING OF THE PLASMA

The analyses of the reactor plasma were zero dimensional, and yielded only the magnitudes of the charged particle power, ion currents, and the electron current. This necessitated some assumptions about the statistics of the ions and electrons escaping through the divertor. The populations were assumed to be Maxwellian with temperatures T_e and T_i. The ratio T_e/T_i was left as a parameter which was studied over the range $1.0 \geq T_e/T_i \geq 0.25$. The Maxwellian plasmas were assumed to be accelerated through an ambipolar potential of $4.5\ kT_e/q$. By selecting a value of T_e/T_i and combining the preceding assumptions with values for the escaping ion current, electron current, and charged particle power, we determined a distribution for the charged particle energies. The results of supplying these charged particle distributions to the direct converter are discussed in the next section.

IV. CAT-D AND D-^{3}He DIRECT CONVERSION - AS CONTRASTED WITH PRIOR D-T MIRROR RESULTS

The processes by which energy is lost from direct conversion are noted in Table I.

Since prior direct energy conversion studies for D-T mirror reactors constitute the bulk of the presently available results, it may be useful to point out the major differences that resulted from the switch to Cat-D and D-^{3}He fuels.

- The mean ion energies are lower and charge-exchange neutralization is no longer negligible. A direct-conversion efficiency decrease of as much as 10% is attributed to charge-exchange in many of the cases.
- The electron energy is higher, over the assumed range of T_e/T_i, and since electron energies are not recovered, the direct conversion efficiency will be decreased.
- The grounded grid size has to be increased to accommodate the higher electron energy that is deposited there. The larger grounded grids intercept more ions before they can reach the collector. The grids contribute more to the efficiency decreases seen in these studies than was attributed to the grounded grid in prior Mirror studies.
- Large D_2 and ^{3}He gas flows must be pumped out of the expander tank. Since conventional cryogenic systems pump D_2 well, but pump He (and by assumption ^{3}He) very poorly, some portion of the pumping surface had to be occupied by diffusion pumps. Because these diffusion pumps pump D_2 gas with less speed than the cryogenic pumps, the D_2 is pumped at a reduced speed, and the background D_2 concentration and the associated charge-exchange neutralization are increased.

Table 1 - The various energy loss mechanisms and the resulting heat depositions are listed.

1)	Charge-Exchange Neutralization: Ions from the reactor are changed into energetic neutral atoms before reaching the collector.	Energetic neutrals give up energy by colliding with electrodes, principally the collector. Resulting low energy ions strike the grounded and negative grids.
2,3)	Electron and ion interception on the grounded grid.	The grounded grid is heated.
4)	Ion interception on the negative grid.	The negative grid is heated.
5)	Ion energies in excess of the ambipolar potential ("ideal collection loss").	The collector is heated.
6)	Collector voltage lowering to accommodate: a) finite magnetic field expansion b) transverse deflection of ion as it passes near a grid.	The transverse velocity component of the ion delivers its energy to the collector as heat.
7)	Thermionic emission from the negative grid: 7G) Current flow to the collector results 7C) Current flow to the collector results	The emitted electrons travel to the grounded grid and the collector where they deposit their energy as heat.
8)	Secondary emission from the negative grid.	Secondary electrons give up their energy to the grounded grid as heat.
9)	Coolant pump power to the grounded grid.	The resulting heat is extracted along with the grid wire coolant.
10)	Structural elements intercept plasma.	The structures which support the direct converter electrodes are heated.

Fig. 4 and Fig. 5 plot, in a cumulative fashion, the contributions of the various loss processes: Fig. 4 for the Cat-D, low-β design[1] and Fig. 5 for the D-^{3}He [1], 1:1, high-β design. These are representative examples. Two different collection losses are listed, that of a single stage collector and that of a 4-stage collector. The two lowest curves represent the direct conversion efficiencies (directly converted electrical power/charged-particle power) for these two designs.

It is interesting to note that for large T_e/T_i, the ion energies (per ionic charge) are closely grouped near the ambipolar potential, and the four-stage collector offers only a few percent improvement over the single stage design. For smaller T_e/T_i, the single stage collector is less efficient, and a four-stage design offers a 10% to 20% improvement in direct conversion efficiency.

The loss processes listed in Table 1 result in the production of heat. Most of this heat can be collected and sent to a thermal bottoming cycle. By assuming that the efficiency of this cycle is 40%, one can calculate a plant efficiency (total power out) for the charged particle power such as is shown in Fig. 6, for a Cat-D design. Fig. 8 shows an outline (top view) of this reactor with attached direct converter tanks. The total charged particle power and the assumed power density determine the expander tank size. Fig. 7 and Fig. 9 show the same results for a D-^{3}He design.

The increase in total electrical power out, which occurs in some cases between 100 W/cm^2 and 150 W/cm^2, is a result of the grid selection process. Radiatively cooled grids whose thermal output can be recovered only in part are used at lower power densities. In the case of the convectively cooled grids used at power densities above 100 W/cm^2, all the thermal power can be recovered and sent to the bottoming cycle.

V. EXTRACTING MAGNETIC FIELD LINES

The toroidal magnetic field lines can be bent and thereby directed through the reactor blanket and shield by bundle diverter coils. The continued radial travel of these lines, in the manner shown in Fig. 10, depends upon two additional coil systems.

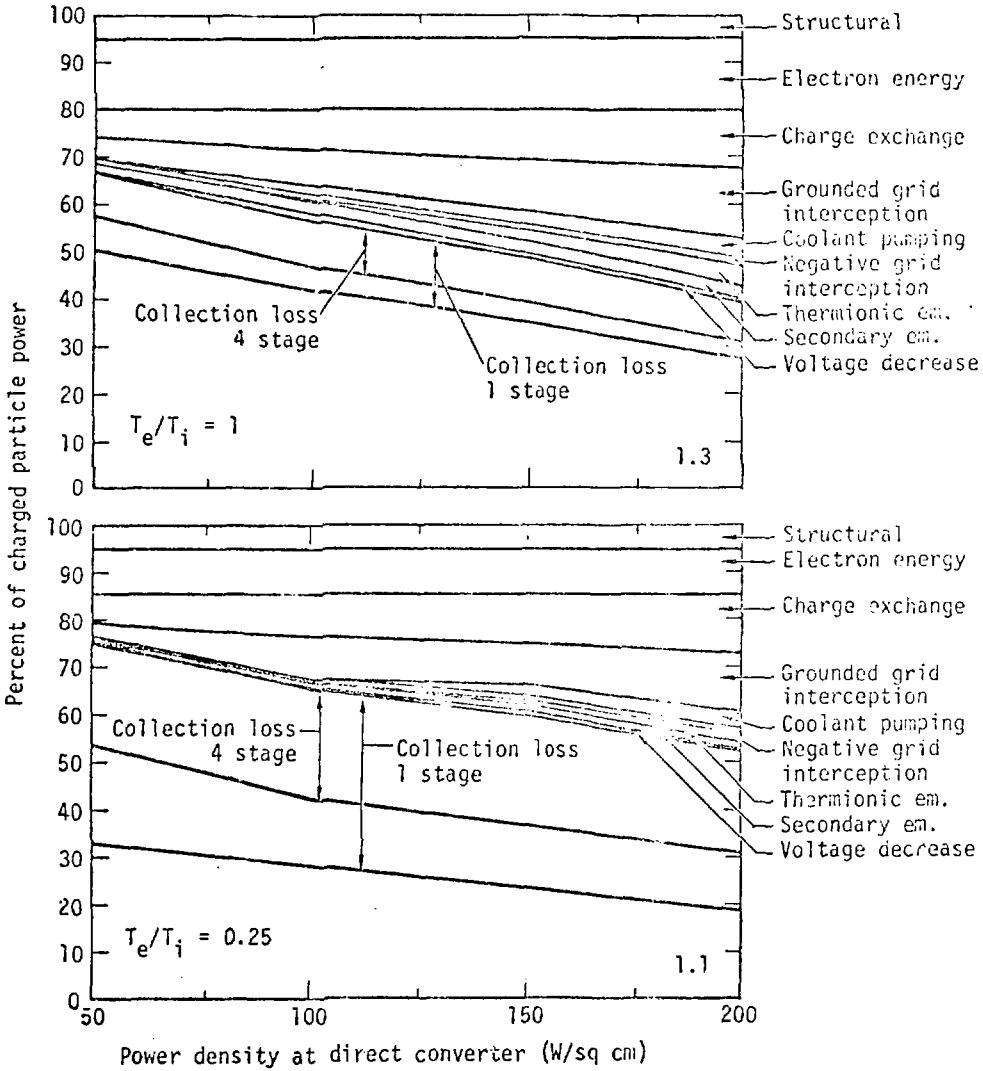

Figure 4. The losses for the low-β, Cat-D design are cumulatively plotted. The upper figure is for $T_e/T_i = 1$; the lower figure is for $T_e/T_i = 0.25$.

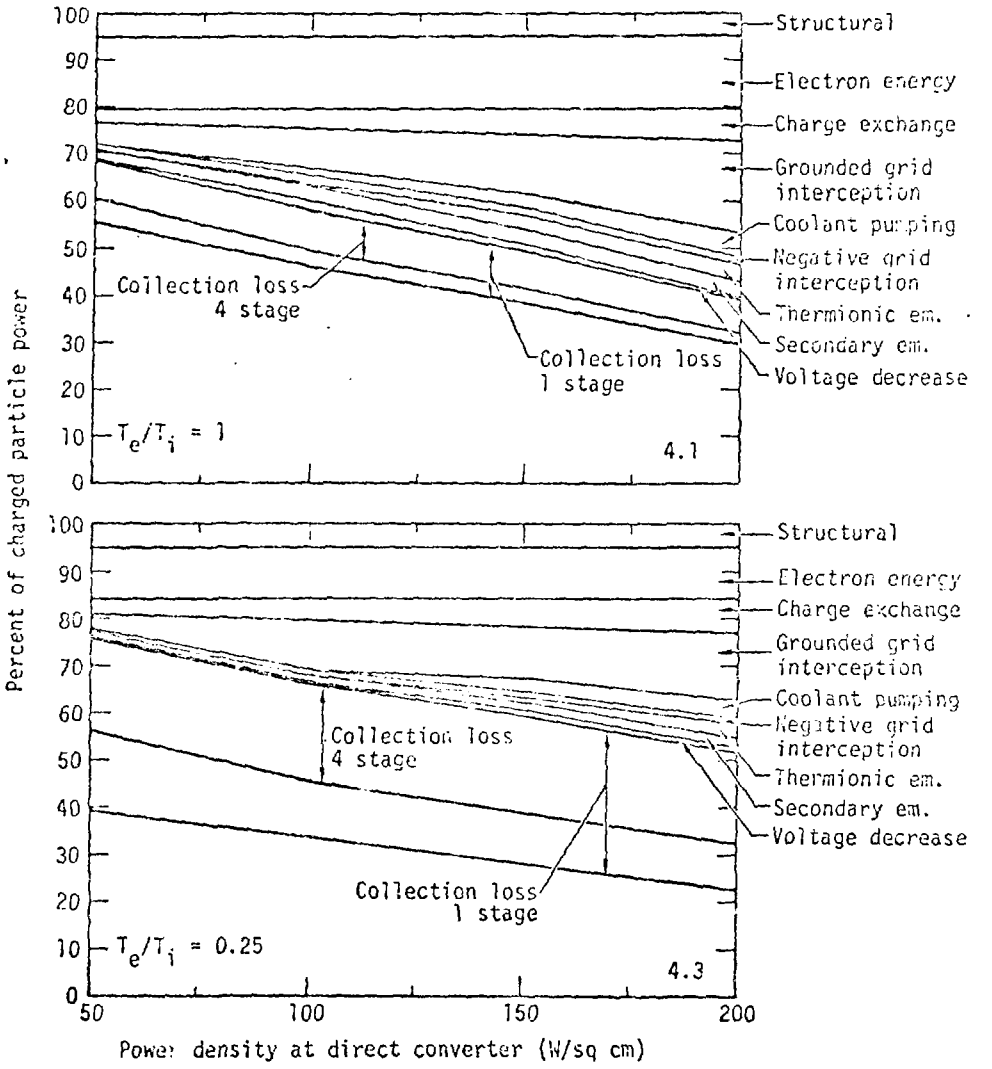

Figure 5. The losses for the D-^{3}He, 1:1 high-β design are cumulatively plotted. The upper figure is for T_e/T_i = 1; the lower figure is for T_e/T_i = 0.25.

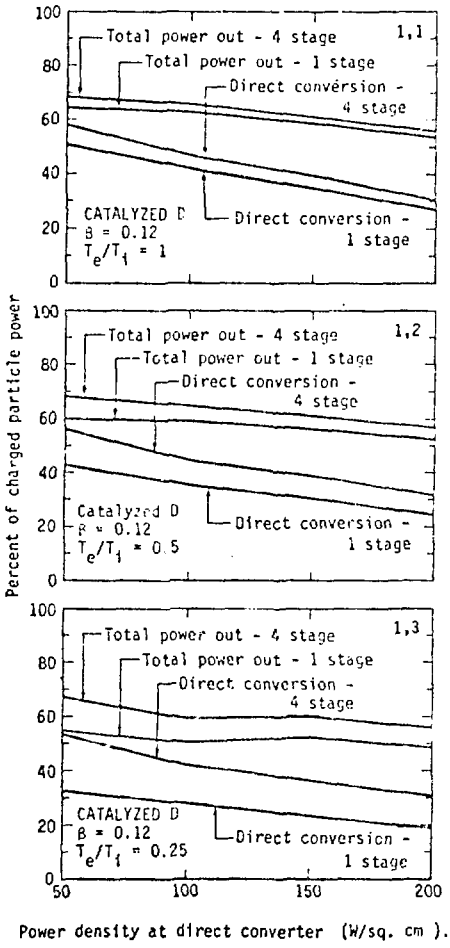

Figure 6.

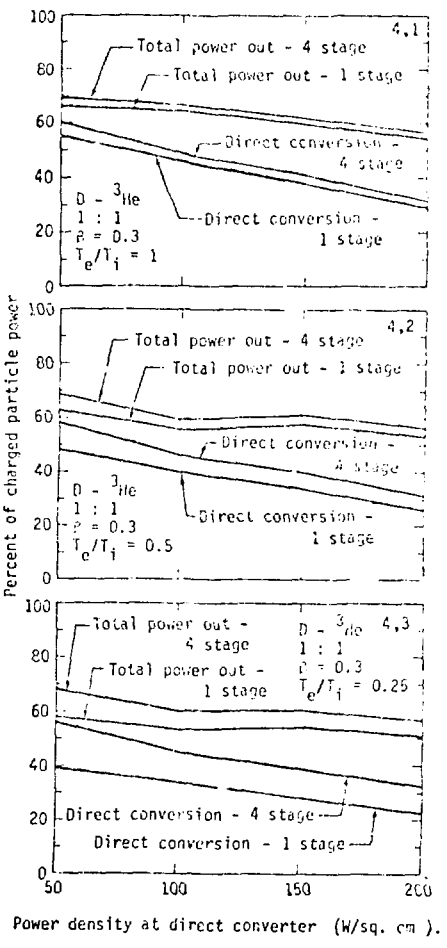

Figure 7.

The direct conversion efficiency and the total electrical power (extracted from the charged particles), assuming a 40% efficient thermal bottoming cycle.

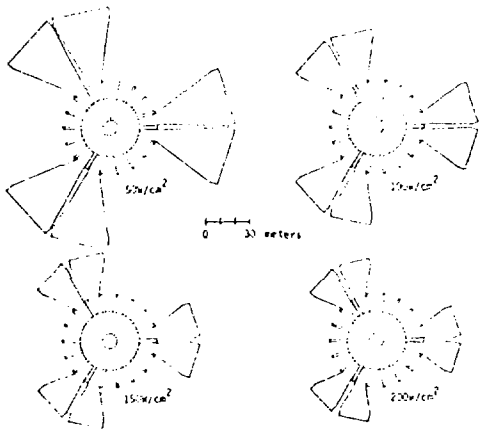

Figure 8. A top-view outline of the Cat-D, low-β reactor and direct converter tanks for differing power densities at the direct converters.

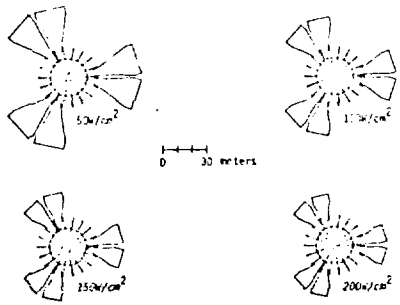

Figure 9. A top-view outline of the D-^{3}He, 1:1, high-β reactor and direct converter tanks for differing power densities at the direct converters.

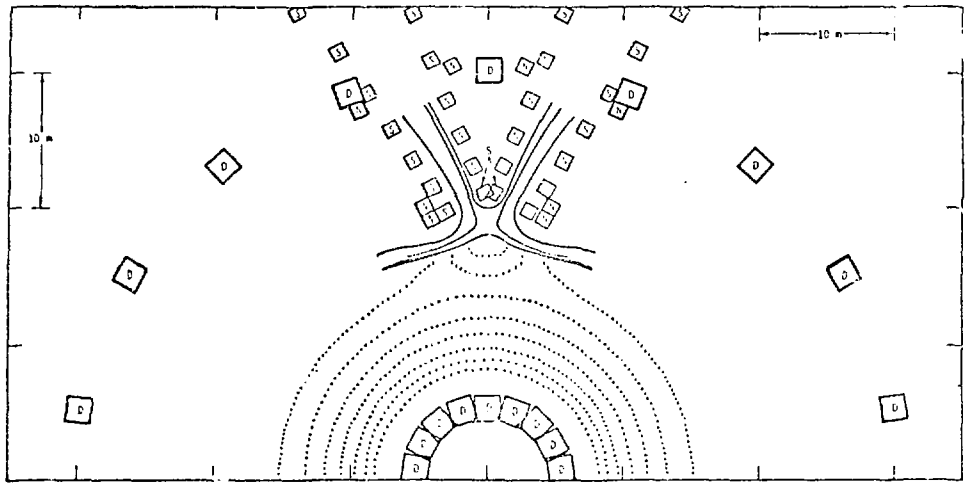

Figure 10. The magnetic field lines (solid curves) are bent into a radial direction by the ring coils, denoted by an s, and the toroidal field nulling coils, denoted by an n.

First, in addition to the bundle diverter coils, a series of ring-like coils, as shown in Fig. 11b, must be spaced along the expander to provide an expanding cone of lines inside. The squares marked s, in Fig. 10, denote sections through these coils.

Second, the toroidal field which cuts through the expander must be canceled. The coils shown in Fig. 11a perform this task. This arrangement surrounds the portion of the expander within the toroidal field. The squares marked N in Fig. 10 denote sections through these coils.

VI. HELIUM PUMPING

For the purpose of this study, it has been assumed that diffusion pumps will be used to remove the large flows of ^3He gas. On the other hand, cryogenic pumps would allow structural simplifications, higher pump speeds, and freedom from back streaming. For this reason we have investigated their application to our He pumping requirements. Only very preliminary results are available, but it now appears that when combined with an N_2 or Ar gas spray, ^4He can be pumped at speeds

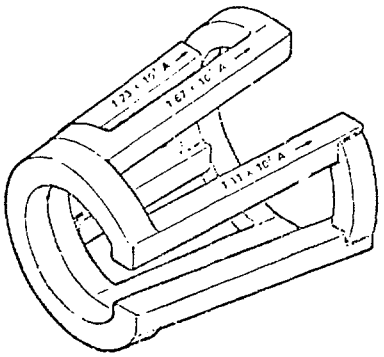

Figure 11a. The toroidal field nulling coil surrounds the portion of the expander within the toroidal field.

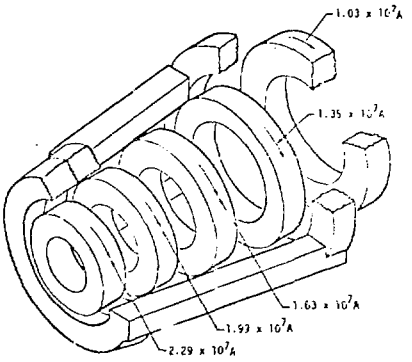

Figure 11b. The ring coils are enclosed by the TFNC.

approaching that with which cryogenic pumps remove D_2[2]. No back streaming of t $_2$ or Ar gases were observed. Experimental work on ^{3}He is now beginning.

VII. NEUTRAL BEAM HEATING

Neutral beam heating is required only during startup. By the nature of the startup procedures, the power requirements are modest: 100 MW for 62 sec. (this worst case corresponds to the high-β Tokamak startup). In order to penetrate the plasma, ion energies of 200-350 keV are required. D and T beams at these energies can be produced at high efficiency by accelerating negative ions, D^- or T^-, and then neutralizing them via photodetachment or stripping in a cesium vapor cell. For these two methods of neutralizing negative ions, the percent ratio of -- neutral beam power to line power into the power supply -- is shown in Fig. 12[3] and Fig. 13[3].

---

[2] This work is being performed by Dr. Thomas Batzer, Lawrence Livermore Laboratory.

[3] J. H. Fink, W. L. Barr, and G. W. Hamilton, UCRL-52173, Nov. 1976.

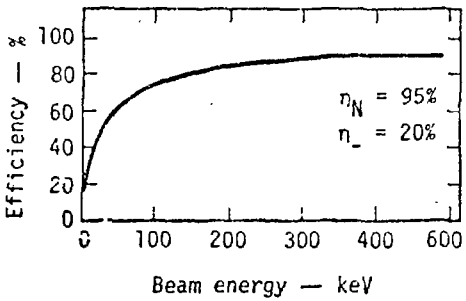

Figure 12. Deuterium neutral beam injection efficiency using negative ion acceleration and photodetachment.

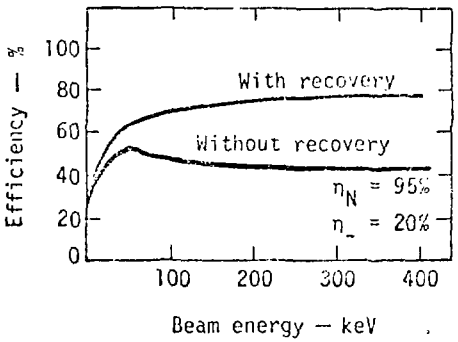

Figure 13. Deuterium neutral beam injection efficiency using negative ion acceleration and cesium cell stripping. Energy recovery includes both direct and thermal energy recovery.